RECONSTRUCTION OF BUILDINGS FROM INTERFEROMETRIC SAR DATA OF BUILT-UP AREAS

U. Soergel, U. Thoennessen, U. Stilla

FGAN-FOM Research Institute for Optronics and Pattern Recognition
76275 Ettlingen, Germany

soe@fom.fgan.de

Commission III

KEY WORDS: SAR, Interferometric SAR, building reconstruction

ABSTRACT:

The improved ground resolution of state of the art synthetic aperture radar (SAR) sensors suggests to utilise such data for the analysis of urban areas. Approaches for a 3D reconstruction of buildings from SAR or InSAR showed good results for rural areas or large and flat buildings, like industrial halls. The situation is more difficult in inner city areas with high buildings which are often located in close proximity to each other. The inherent oblique scene illumination by SAR results in occlusion of objects by more elevated objects interrupting the line of sight. Another problem is the mixture of signal contributions of different objects with the same distance to the sensor. Furthermore, specular reflection and multi-bounce scattering can result in very strong signals which superimpose the backscatter of large parts of their neighbourhood. Geometric constraints of the impact of the mentioned SAR phenomena on the visibility of buildings are derived. The opportunities and limitations of remote sensing of inner city scenes with radar are discussed by comparison of real InSAR data with ground truth like maps and high resolution DEM. An approach for the detection and reconstruction of buildings from InSAR data is proposed and demonstrated.

1. INTRODUCTION

The increasing resolution of SAR sensors opens the possibility to utilize such data for scene interpretation in urban areas. Approaches for a 3D building recognition from SAR and InSAR data have been proposed for rural areas [Bolter, 2001], industrial plants [Soergel et al., 2001] and inner city areas with high buildings [Gamba et al., 2000]. It turned out that different SAR specific phenomena [Schreier, 1993] like foreshortening, layover, shadow and multipath-propagation burden the scene interpretation or make it even impossible. These phenomena arise from the side-looking scene illumination of SAR sensors. The mentioned methods from the literature achieved good results for rural areas or large and detached buildings. Especially in dense built-up areas with high buildings, large portions of the data can be interfered by the illumination effects.

However, even in dense urban environment a building recognition is feasible, if the typical appearance of buildings in the data is properly modelled. It is e.g. possible to determine the height and the roof structure from the length and the size of the occluded shadow area cast from the building on the ground behind. Other hints to buildings are layover areas and bright double-bounce scatterers at the building footprint. Such context knowledge is exploited by a novel model-based iterative approach to detect and reconstruct buildings.

First, we introduce briefly in Chapter 2 the acquisition of InSAR data. The appearance of buildings in SAR images is discussed in Chapter 3. Phenomena caused by side-looking illumination are explained and geometric relations for the determination of disturbed data are derived. The model-based approach for the detection and reconstruction of buildings is proposed in Chapter 4.

2. INSAR DATA

Side-looking SAR sensors are mounted on satellites or airplanes. The basic sensor principle is to illuminate large areas on the ground with the radar signal and to sample the backscatter. From the different time-of-flight of the incoming signal the range between the sensor and the scene objects is obtained. The analysis of single SAR images is usually restricted to the signal amplitude.

SAR interferometry (InSAR) takes benefit from the coherent SAR measurement principle. For airborne single-pass across-track interferometry measurements two antennas are mounted perpendicular to the carrier track with a geometric displacement. One antenna illuminates the scene and both antennas receive the backscattered complex signals. An interferogram is calculated by a pixel by pixel complex multiplication of the master signal with the complex conjugated slave signal. Due to the geometric displacement, the distances from the antennas to the scene differ, which results in a phase difference in the interferogram. Considering the distance, wavelength, antenna geometry, and viewing angle elevation differences can by calculated from the phase difference.

The accuracy of a DEM produced with the InSAR technique varies locally depending on the signal to noise ratio (SNR). The so called coherence is a measure of the local SNR. Coherence is usually estimated from the data by a window-based computation of the magnitude of the complex cross-correlation coefficient of the SAR images. The noise sensitivity results often in data holes or competing elevation values after the geocoding with the forward transformation. Hence, the InSAR height data has to be further processed before the geocoding step is carried out.

Figure 1 illustrates the InSAR data set of the test site in ground range projection. The data were recorded by the airborne AER-II experimental multi-channel SAR system [Ender, 1998]. This system is equipped with a phased array antenna and several receiver channels. The center frequency of this X-band system is 10 GHz (λ = 3cm) with bandwidth of 160 MHz. The ground range data has a approximate resolution of 1m x 1m. Range direction is from top to down. Assuming a constant noise power, it is evident that in areas with low backscatter power the SNR is poor. This results in a low coherence (Figure 1c) and distorted height data (Figure 1b).

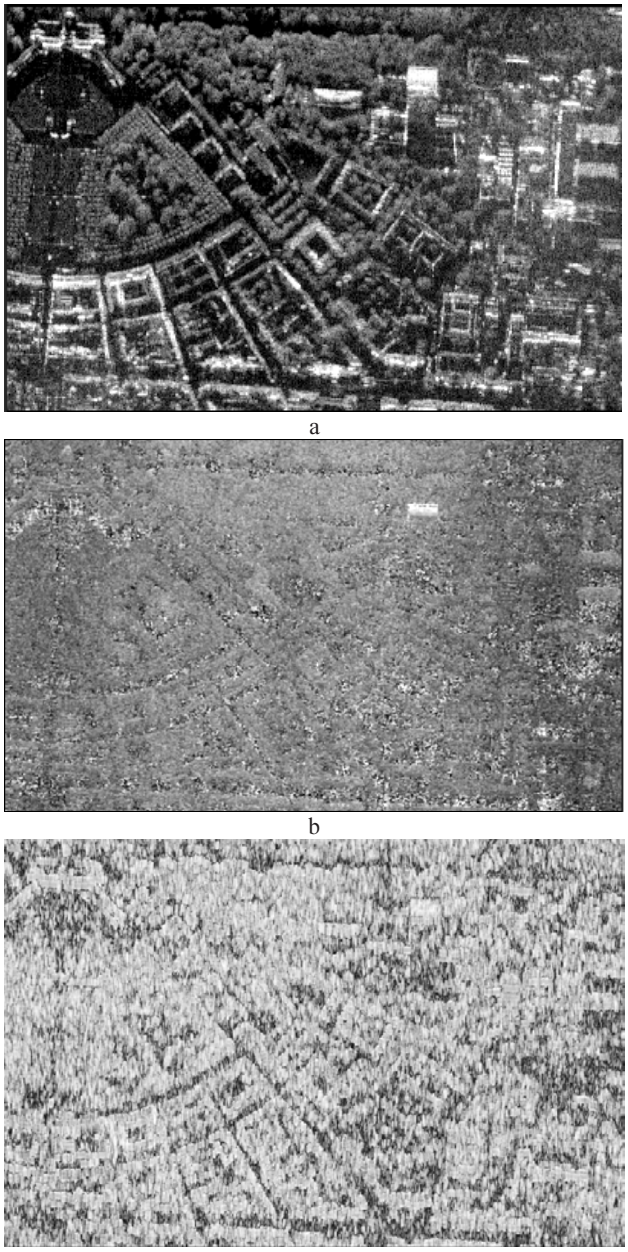

a

b

c

Figure 1. InSAR data set of test site Karlsruhe . a) intensity, b) height, c) coherence (bright = high SNR)

3. APPEARANCE OF BUILDINGS IN SAR IMAGES

3.1 Phenomena caused by side-looking illumination

Figure 2 illustrates typical effects in SAR images in the vicinity of buildings. The so-called layover phenomenon (Figure 2a) occurs at locations with steep elevation gradient facing towards the sensor, like vertical building walls. Because object areas located at different positions have the same distance to the sensor, like roofs (I), walls (II) and the ground in front of buildings (III), the backscatter is integrated to the same range cell. Layover areas appear bright in the SAR image (Figure 2 c).

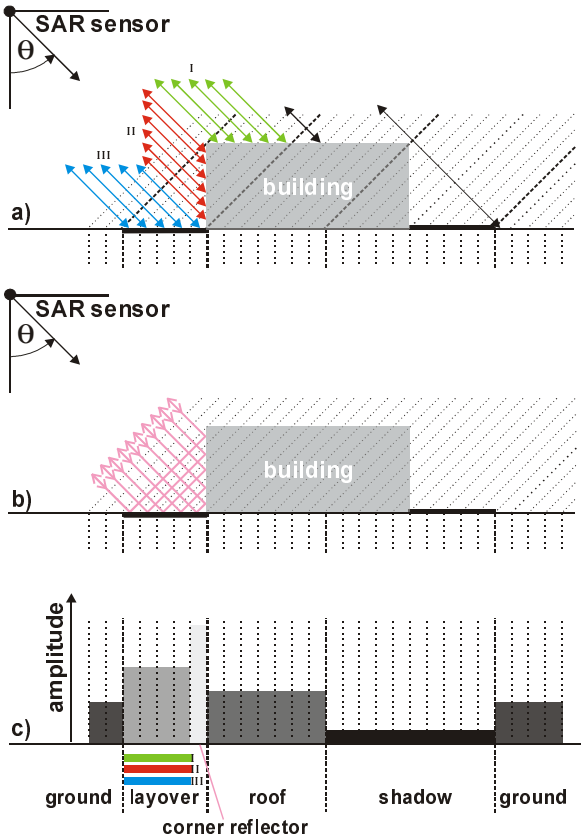

Figure 2. SAR Phenomena at a flat roofed building. a) layover, b) corner reflector, c) range line of SAR image.

Perpendicular alignment of buildings to the sensor leads to strong signal responses by double-bounce scattering at the dihedral corner reflector between the ground and the building wall (Figure 2b). This results in a line of bright scattering in azimuth direction at the building footprint (Figure 2c). At the opposite building side the ground is partly occluded from the building shadow. This region appears dark in the SAR image, because no signal returns into the related range bins.

Roof structures may lead to strong signal response as well. Since the entire power is mirrored back to the sensor this reflection leads to a line of dominant scattering in azimuth direction, similar to the corner reflector. This bright line caused from the roof appears closer to the sensor in the SAR image compared to the corner reflector. Besides the offset in range direction both effects can be discriminated by their polarimetric properties (single-bounce respectively double-bounce).

The mentioned effects can be studied in Figure 3 comparing a section of an aerial image and a SAR image (the castle at the upper left side in Figure 1a). The SAR image is superimposed with the building footprints from a map. The scene was illuminated from top. The signal from the corner reflector at the castle's main building is located at the building footprint (1). The bright signal from the gabled roof is projected on the terrace in front of the castle (2). These two lines enclose the layover area. Layover can be observed as well at the castle wing

(3) and at the tower (4). At the wing no line of bright scattering appears, because the double-bounce signal is reflected away from the sensor. Another double-bounce event happens at a little wall at the border of the terrace (5).

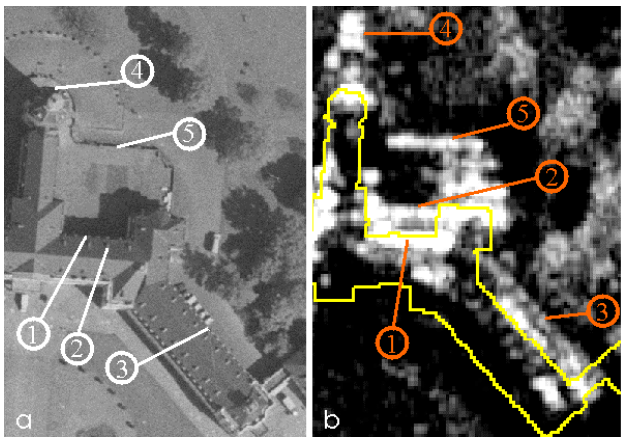

Figure 3. Karlsruhe Castle: a) aerial image (1 main building wall, 2 main building roof, 3 wing, 4 tower, 5 terrace wall), b) SAR image overlaid with building footprints (yellow) and pointers to SAR phenomena (orange), SAR illumination from top to down

3.2 Geometric Constraints

The phenomena of layover and shadow are discussed in more detail. The sizes of the layover areas l_g and shadow areas s_g on the ground in range direction depend on the viewing angle θ and the building height h. The layover area (see Figure 4a) is given by:

$$l_g = h \cdot \cot(\theta). \quad (1)$$

For the buildings analysis the roof area l_{rt} is of interest which is influenced by layover. At the far side of a building with width w a part of the roof is not interfered with layover (shown in green in Figure 4a), if the inequation is fulfilled:

$$h < w \cdot \tan(\theta). \quad (2)$$

In case of shadow geometric relations can be obtained, too (Figure 4b). The slant range shadow length Δr is the hypotenuse of the rectangular triangle with the two sides h and s_g. Hence, the building elevation h is given by:

$$h = \Delta r \cdot \cos(\theta). \quad (3)$$

A simple projection of the slant range SAR data on a flat ground plane (ground range), ignoring the building elevation, leads to a wrong mapping of the roofs edge r_1 to point r_1'. Starting from point r_2 the true position x1 of the building wall can be determined:

$$x_2 = r_2 \cdot \sin(\theta) \quad (4)$$

$$x_1 = x_2 - \Delta r \cdot \sin(\theta) \quad (5)$$

$$s_g = x_2 - x_1 = h \cdot \tan(\theta). \quad (6)$$

However, the shadow analysis can be reliable only if the ground behind the building is flat and if no signal from other elevated objects interferes the shadow area (e.g a neighbored building). It is obvious, that at building locations a steep viewing angle θ leads to large layover areas on the ground and the roofs, but to small shadow areas and vice versa. Therefore, the viewing angle has to be chosen carefully in order to maximize the portion of useful SAR data.

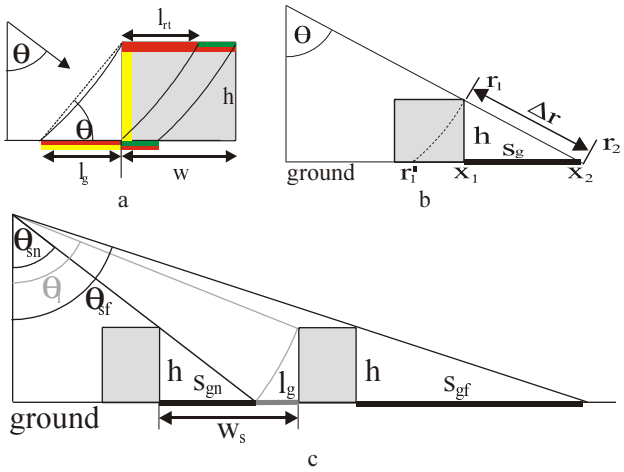

Figure 4. a) Layover in front and on a flat roofed building, b) Shadow behind a building, c) Shadow and Layover from buildings displaced in range direction.

The viewing angle increases in range direction over the swath. Assuming a range of the viewing angle θ between 40° and 60°, the shadow length of a certain building is more than doubled from near to far range. In Figure 4c such a situation is depicted (shadow length s_{gn}, s_{gf}). A worst case will arise if a road between two building rows is orientated parallel to the sensor trajectory. The street is partly occluded from shadow and partly covered with layover. An object on the road can only be sensed properly, if a condition for the road width w_S holds:

$$w_s > s_{gn} + l_g = h \cdot (\tan(\theta_{sn}) + \cot(\theta_l)). \quad (7)$$

3.3 Simulation of layover, shadow and dominant scattering at buildings

Based on a ground truth DEM it is possible to simulate layover and shadow areas (Meier et al., 1993) as well as dominant scattering. Such a simulation was carried out for the test site according to the given parameters of the real SAR data. A detailed visibility analysis reveals that only 20% of the road area and 43% of the roof area can be sensed properly with this SAR measurement. The rest is interfered with layover, shadow or both. A fusion of complementing SAR data acquired from different aspects offers the opportunity to fill occluded areas and to correct layover artefacts. SAR simulation techniques are incorporated in the iterative building detection and reconstruction approach presented in the next chapter.

4. APPROACH FOR BUILDING DETECTION AND RECONSTRUCTION FROM INSAR DATA

In this chapter an approach for building detection and recognition from InSAR data is described. Based on the used imagery the concept for the assessment of the results shall be discussed first.

4.1 Imagery and Ground Truth

A section of the captured test site (Karlsruhe, Germany) is shown in Figure 5. During the SAR measurement an aerial image in oblique view was taken (Figure 5a). The corresponding InSAR intensity and height are depicted in Figure 5c,d. For better comparison with the aerial image (Figure 5a) the SAR image were rotated by 180 degree (comp. Figure 1). The range direction is now bottum-up. The InSAR data is still in slant range geometry, with a better resolution in azimuth direction (horizontal coordinate). Figure 5e shows again the intensity image overlaid with the building footprints drawn by a human operator without any context information of the scene. This information shall be called "sensed truth". The comparison with the LIDAR DEM (Figure 5f) and the aerial image in nadir view (Figure 5b) reveals that even a human operator cannot spot every building in the scene.

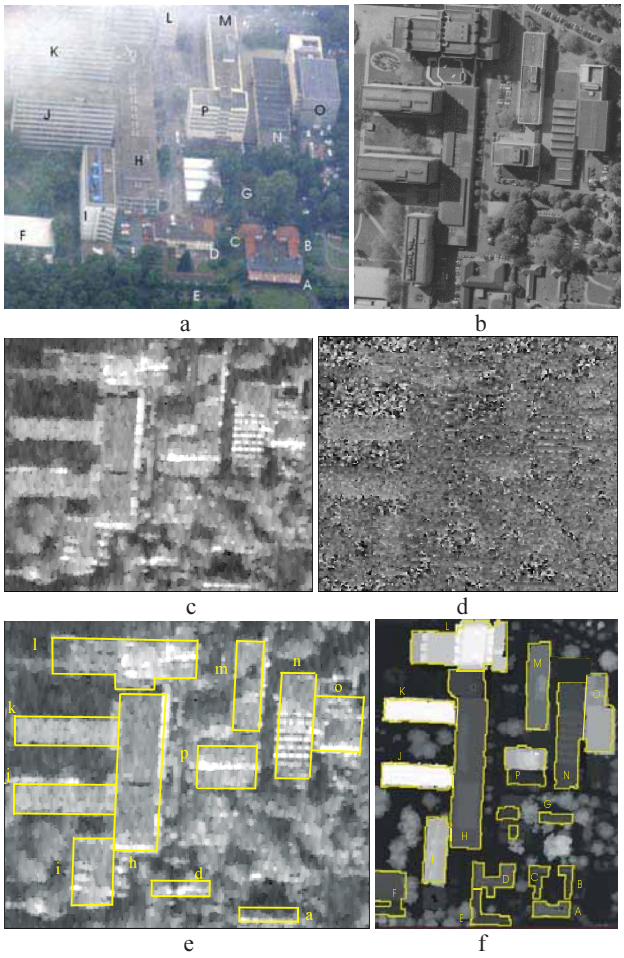

Figure 5. a) aerial image shot during InSAR measurement, b) aerial image in nadir view, c) InSAR intensity in slant range, d) InSAR height in slant range, e) "sensed truth", f) LIDAR data and "ground truth".

Especially small buildings are hardly visible or buildings which are covered by layover e.g. from high trees. Scene interpretation from remote sensing imagery is a demanding task. The human ability to interpret even complex scenarios is usually not accomplished by automatic machine vision systems. Hence, the sensed truth represents a best effort result of any automatic approach.

The assessment of the building detection is carried out in a twofold manner. The performance of the proposed approach will be assessed with respect to the sensed truth. Furthermore, it is interesting to compare the results with the ground truth (Figure 5f). The latter gives insight in the feasibility of building detection and reconstruction with this approach using InSAR data of the given quality.

4.2 Algorithm overview

The building recognition is performed in an iterative manner. Detection and reconstruction of buildings is carried out in separated modules. The first step is the preprocessing of the InSAR data (e.g. smoothing and speckle reduction [Desnos and Matteini, 1993]). In the following segmentation step primitive objects are extracted from the original slant range InSAR data. This is advantageous in order to avoid artefacts due to the geocoding, e.g. the distorted appearance of building edges in the ground range projection. From primitive objects more complex objects (building hypotheses) are assembled in the detection step. After projection of coordinates of these building candidates from slant range into word coordinate system, a building recognition step follows. In this step model knowledge is exploited, e.g. rectangular shape of buildings or preferred parallel alignment of buildings along roads. Intermediate results are used for a simulation of layover, shadow and dihedral corner reflectors. The simulation results are re-projected to the SAR geometry and compared with the real data. Differences between the simulation and the real data steer the update of the process: new building hypotheses are generated and false ones eliminated. Hence, the resulting scene description is expected to converge to the real 3D objects in the scene with increasing number of steps.

4.3 Segmentation of primitive objects

Primitive objects are segmented in the intensity data and the height data.

4.3.1 Intensity Data: In the intensity data edge and line structures are detected. There are mainly three types of structures of interest:

- Salient bright lines caused from layover or double-bounce reflection. Those objects will be referred as objects STRONG_SCATTER_LINE.
- Edge structures at the border of a dark region which are potentially caused from building shadow. Two sets of objects are distinguished. The first set build those border edges of the dark region which face the sensor (object NEAR_SHADOW_EDGE). The other set consists of the edges at the far side of the dark region (object FAR_SHADOW_EDGE).
- The remaining edges build the set of other objects BUILDING_EDGE. Those may coincide with building edges orientated in range direction.

4.3.2 Height Data: In the height data a segmentation of objects with significant elevation above ground is carried out. For this purpose a normalized DEM (NDEM) is derived from the InSAR height data, which represents the elevation of objects over ground. First a rank filtering of the height data is performed. The filter window size is chosen larger than the expected maximum building area. Height values coinciding with poor coherence or low intensity are not considered in this step in order to exclude blunders. This filtering results in a digital terrain model (DTM) representing the topography

without elevated objects like trees or buildings. The NDEM is derived from the difference of the original InSAR height to the DTM. With an elevation threshold elevated objects are separated from the ground in the NDEM. Connected regions of elevated pixels build the set of objects ELEVATED_REGION.

4.4 Detection of Building Candidates in the Slant Range

From the line and edge structured primitive objects more complex objects QUADRANGLE are assembled by a production system:

- At least one edge of the object QUADRANGLE facing the sensor must be derived from an object STRONG-SCATTER_LINE.
- Analogous, an object NEAR_SHADOW_EDGE is required at the far edges of the object quadrangle.

The objects QUADRANGLE from the test data are shown in Figure 6. Only a subset of those coincide actually with buildings. A variety of different object configurations are source of false hints, e.g. fences or car rows etc.

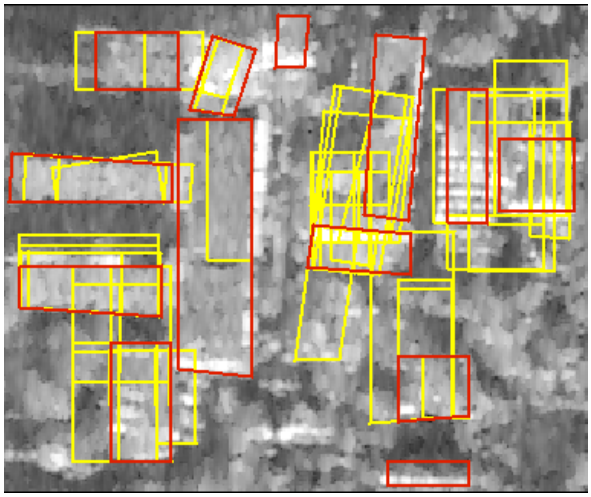

Figure 6. The set of all assembled objects quadrangle. The elevated and best assessed subset form the objects BUILDING_CANDIDATE (red)

For the discrimination of buildings from the rest the objects ELEVATED_REGION are used. The intersection area of each object QUADRANGLE with all objects ELEVATED_REGION is determined. The ratio of the intersection area to the quadrangle area is used as object feature “elevated area ratio”. Only objects QUADRANGLE with an elevated area ratio larger than 0.7 are considered as objects BUILDING_CANDIDATE. The number of objects BUILDING_CANDIDATE is further reduced: from mutual intersecting candidates only the best assessed one is considered for the reconstruction step in this iteration. The assessment value depends on:

- the overlap and the parallelism of the primitive objects
- the feature “elevated area ratio”.

In Figure 6 the remaining objects BUILDING_CANDIDATE of the first iteration are drawn in red.

4.5 Building Reconstruction

The building reconstruction is based on the following scene model:

- Footprints of buildings have rectangular or right-angled shape.
- Buildings are elevated objects with different roof structures. Three types of parametric building models are considered: flat roof buildings, gabled roof buildings and pent roof buildings. A common feature of the parametric building models is the rectangular footprint.
- A generic building model addresses complex buildings structures which consist of several parts like wings. These parts may have different height which is constant for each part. The footprint of a generic building is modelled as a right-angled polygon. The number of parts of a generic object is not a-priori determined.
- Neighboured buildings and the parts of complex buildings have often the same orientation, because they are aligned parallel to roads.

For the reconstruction step the coordinates of the objects BUILDING_CANDIDATE are transformed from the SAR geometry into the word coordinate system. This step requires knowledge of the object height. A pixel by pixel transformation leads to distorted object edges, due to the noise sensitivity of the interferometric measurement. The noise impact is reduced by averaging the height values inside the borders of each object BUILDING_CANDIDATE. In case of a flat roofed building, the average value is the optimal estimate of the building height. In order to consider the different reliability of the height pixel values, the related coherence value is used as weight in the averaging procedure.
Because of tolerances in the building candidates assembly, the building footprint is usually not right-angled after geocoding. Therefore, the footprint is approximated by a rectangular or right-angled polygon. The roof structure is analysed with two different methods. The first method is restricted to the height data. After the re-projection of the right-angled building into the slant range, planes are fitted to the data. The second method analyzes the size and shape of the shadow areas (objects NEAR_SHADOW_EDGE and FAR_SHADOW_EDGE). Both results are combined to determine the roof shape and to improve the footprint location. The corrected footprint and roof structure are features of new produced objects BUILDING.

4.6 Iterative improvement of the results

The first iteration is restricted to the reconstruction of objects BUILDING with rectangular footprints. In the following iterations the generic building model is considered as well. If several InSAR data sets are analyzed, the results are fused. In case of competing results, only the object BUILDING with the best assessment is accepted for the fused result. Occluded areas are filled and layover effects compensated. Due to parameter tolerances, the reconstructed orientations of neighboured objects BUILDING might differ slightly. Hence, the orientations are corrected. The assessment of the objects buildings are used as weight for this adjustment step. Based on the intermediate results simulations of layover, shadow and dihedral corner reflectors are carried out with respect of the parameters of the real data. Differences between the simulation and the real data are hints to inconsistencies. These govern the update of the process: new building hypotheses are generated and false ones eliminated. Then the reconstruction step is repeated.

5. RESULTS

The result of the first iteration re-projected into the slant range after the reconstruction step is illustrated in Figure 7a (red rectangles). The shadow analysis did not yield good results, due to the proximity of the buildings and many trees in the scene. Therefore, the calculation of the building height based mainly on the InSAR height data. 13 buildings were detected. The result is assessed with respect to the two sets of ground truth data (Figure 5e,f).

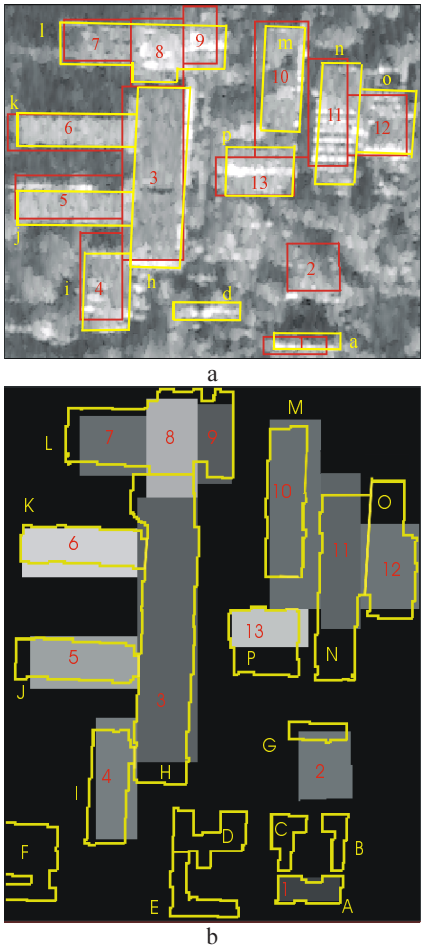

Figure 7. a) Result of first iteration re-projected into the slant range after the reconstruction step (red) and sensed truth, b) final result after 5 iterations (grey value coding of building height) superimposed with real ground truth.

The comparison with the sensed truth (yellow in Figure 7a) gives: 9 buildings are correct, one is missing (d) and one is over-segmented (l). The over-segmentation was caused from superstructures on the rooftop with significant different height. One false building is present (object 2) at the location of large trees. However, the mayor part of those buildings were detected which were labelled manually.

In Figure 7b is the final result after five iterations illustrated. The grey level corresponds with the reconstructed building height. The real ground truth is superimposed in yellow. With respect to this ground truth, additional five buildings at the bottom of the scene are missing. The reason is in most of the cases occlusion or layover caused from high trees. Building G for example is not visible at all even in the aerial image shown in Figure 5a. However, mainly small buildings were not detected. Especially the height of tall buildings was underestimated. The buildings J and K on the left hand side are about 40 m high. But, their estimated height was 7 m smaller. A wrong height estimate leads to a erroneous position of the footprint after the forward transformation into the world coordinate system. The buildings appear shifted towards the sensor. The main parts of the two building complexes were detected. The recognition of the gabled roof of the small building A failed. It was reconstructed as flat roof building. Probably, this roof would not be reconstructed correct from this InSAR data set even in case the building was detached. The reason is the orientation of the building in azimuth direction which is disadvantageous for the shadow analysis. For a illumination from the right, better results could be expected.

6. CONCLUSION

The derived geometric relations show that always some parts of the urban scene can not be sensed by a single SAR measurement. This behaviour is caused from the inherent side-looking illumination by SAR. The results of the approach confirm that especially tall buildings and trees may cause problem areas, due to occlusion or layover. However, the main buildings could be detected and reconstructed, even for the analysis of the given single InSAR data set. The accuracy of the results can not compete with 3D reconstructions derived from LIDAR data. A potential for the improvement of results offers the fusion of several SAR and InSAR data [Bolter, 2001]. This has to be investigated with focus on dense urban areas. In case of a multi-aspect analysis an iterative approach is particularly suitable, because hints from the one image may initiate a refined analysis at the related locations in the other images.

REFERENCES

Bolter R.: Buildings from SAR (2001) Detection and Reconstruction of Buildings from Multiple View High Resolution Interferometric SAR Data. PhD. thesis, University Graz, Austria.

Desnos Y L, Matteini. V (1993) Review on structure detection and speckle filtering on ERS-1 images. EARSeL Advances in Remote Sensing, 2(2), pp. 52-65.

Ender JHG (1998) Experimental Results Achieved with the Airborne Multi-Channel SAR System AER-II" Proceedings of EUSAR'98, Friedrichshafen: VDE, pp. 315-318.

Gamba P, Houshmand B, and Saccini M (2000) Detection and Extraction of Buildings from Interferometric SAR Data, IEEE Transactions on Geoscience and Remote Sensing, vol. 38, no. 1, pp. 611-618.

Meier E, Frei U, and Nuesch D (1993) Precise Terrain Corrected Geocoded Images. In: Schreier G (ed.) SAR Geocoding: Data and Systems, Wichmann, Karlsruhe, pp. 173-185.

Schreier G (1993) Geometrical Properties of SAR Images. In: Schreier G (ed) SAR Geocoding: Data and Systems. Wichmann, Karlsruhe, pp. 103-134.

Soergel U, Schulz K, and Thoennessen U (2001) Phenomenology-based Segmentation of InSAR Data for Building Detection". In: Radig, B., Florczyk, S. (eds) Pattern Recognition, 23rd DAGM Symposium, Springer, pp. 345-352.